sustainability

MDPI

Article

Acoustic-Gas Coupling Response Law in the Whole Process of Coal and Gas Outburst

Chaolin Zhang [1,2,*], Wei Zeng [1,2], Jiang Xu [3], Shoujian Peng [3], Shan Yin [1,2], Qiaozhen Jiang [1,2] and Mingliang Liu [1,2]

1 Key Laboratory of Gas and Fire Control for Coal Mines (China University of Mining and Technology), Ministry of Education, Xuzhou 221116, China; weizeng@cumt.edu.cn (W.Z.); ysviola@163.com (S.Y.); ts22120150p31@cumt.edu.cn (Q.J.); ts22120165p31@cumt.edu.cn (M.L.)
2 School of Safety Engineering, China University of Mining and Technology, Xuzhou 221116, China
3 State Key Laboratory of Coal Mine Disaster Dynamics and Control, Chongqing University, Chongqing 400030, China; jiangxu@cqu.edu.cn (J.X.); sjpeng@cqu.edu.cn (S.P.)
* Correspondence: chaolinzhang@cumt.edu.cn

Abstract: The intensification of the global energy crisis has led to an increasing demand for coal. China is a major coal-producing country in the world and also the country with the most severe coal and gas outburst disasters. Thus, the coal and gas outburst experiment was conducted, and the following results were obtained: the whole outburst process was divided into three stages, namely the outburst preparation stage, the outburst gestation stage, and the outburst development stage. The gas pressure and acoustic emission signals show significant changes in all three stages, while the variation patterns are different. The gas pressure changes were strongest and the acoustic emission signals were highest during the development stage. Therefore, the outburst development stage was further subdivided into four phases, and the correlation between acoustic emission and gas pressure in each phase was analyzed in detail. Furthermore, the acoustic emission signals in three stages were compared and analyzed. The peak values of acoustic emission count and energy reached 285 times·s^{-1} and 245 V in the preparation stage and reached 265 times·s^{-1} and 231 V in the gestation stage, respectively, only 1.66%~1.78% and 2.19%~2.32% of the development stage, namely 15,980 times·s^{-1} and 10,566 V. Moreover, it was found that the cumulative count and cumulative energy showed a parabolic relationship with the development time of the outburst. Based on the above experimental results, during the production process in coal mines, the dangerous state of outbursts can be monitored through gas pressure changes in the outburst preparation stage and gestation stage. Once in the development stage, more sensitive signals of acoustic emission and their fitting results are used for outburst hazard monitoring and early warning. Monitoring and warning of outbursts of combined gas pressure and acoustic emission signals can effectively improve the safety level of coal mine production.

Keywords: coal and gas outburst; physical simulation test; gas pressure; acoustic emission; acoustic-gas coupling

check for updates

Citation: Zhang, C.; Zeng, W.; Xu, J.; Peng, S.; Yin, S.; Jiang, Q.; Liu, M. Acoustic-Gas Coupling Response Law in the Whole Process of Coal and Gas Outburst. *Sustainability* **2023**, *15*, 12940. https://doi.org/10.3390/su151712940

Academic Editor: Paul Ziehl

Received: 4 August 2023
Revised: 21 August 2023
Accepted: 25 August 2023
Published: 28 August 2023

1. Introduction

With the continuous intensification of the global energy crisis, coal has further attracted worldwide attention [1,2]. Under the backdrop of the goal of carbon neutrality and a carbon peak, China's coal situation has improved year by year. In 2022, China's coal production reached 4.56 billion tons, an increase of 10.5% compared to 2021 and setting a new historical record. China is the country with the most severe coal and gas outburst disasters in the world. According to statistics, a total of 490 coal and gas outburst accidents occurred in China from 2001 to 2021, resulting in 3219 deaths [3,4]. Coal and gas outbursts are a very harmful dynamic disaster phenomenon in coal mines [5–7]. Specifically, a large amount of coal-gas two-phase flow is suddenly emitted into the mining space, such as

roadways and mining faces, in a very short period of time [8,9], which seriously threatens the safety of mine production. During the process of coal and gas outbursts, a large number of acoustic emission signals are generated, and the gas pressure of the coal seam changes significantly. Therefore, the study of acoustic-gas coupling laws can provide a scientific basis for preventing coal and gas outbursts and monitoring coal mine safety hazards [10–12].

Many scholars have done a lot of research on coal and gas outbursts using different research methods. For example, Skochinski et al. [13] carried out coal and gas outburst simulation experiments and analyzed the evolution of gas pressure and emissions during outbursts. Alexeev [14] developed two generations of true triaxial loading apparatuses to simulate outbursts and found that water absorption is higher than about 3%, making the outburst-type fracture mode impossible. Zhang et al. [15] analyzed the relationship between deformed coal, high-energy gas, and coal gas outbursts. They studied the occurrence status of gas in coal seams and explored the degree of damage and thickness of deformed coal controlled by geological structures. Guo et al. [16] conducted orthogonal experiments using a self-designed experimental system. The results showed that the diameter of the outburst mouth had the greatest influence on the intensity and duration of coal and gas outbursts, followed by coal particle size and initial gas pressure. Lu et al. [17] used the triaxial simulation test system to conduct coal and gas outburst experiments under different water content conditions. The moisture content has a direct impact on multiple parameters of coal, which in turn affect coal and gas outbursts. Shi et al. [18] proposed the solid-gas-stress coupling model and conducted numerical simulations of coal and gas outbursts. It was found that the sensitivity of gas content in the outburst process was the lowest among the three main outburst factors. Ding et al. [19] conducted an experimental study on the evolution process of gas outburst, and the results showed that gas pressure, water content, and gas decompression rate had certain effects on gas outburst. Xue et al. [20] studied the application of risk assessment and energy methods to explain the outburst process by using the outburst test device. Cao et al. [21] used a simulation test device for the dynamic effects of coal and gas outbursts to determine the degree of influence of gas adsorption on outburst strength. Zhou et al. [22] used experimental equipment to explore the mechanism of coal oxidation on coal seam outburst risk. Yang et al. [23] found that water injection by blasting can reduce the outburst strength.

Based on previous research results, monitoring coal and gas outbursts is one of the best ways to control their occurrence. Therefore, methods such as acoustic emission (AE) and electromagnetic radiation (EMR) were widely used in monitoring outburst disasters [24–26]. Zheng et al. [27] found that the acoustic emission characteristics of coal varied significantly over different periods. Kong et al. [28] conducted triaxial compression experiments on methane-bearing coal. The results showed that acoustic emission response and fractal dimension can reflect the evolution and growth of cracks during loading. Ali et al. [29] studied the influence mechanisms of water, mechanical properties, and acoustic emission signals on stress–strain curves and SEM results of saturated and dry water samples. The research found that water saturation weakened various mechanical properties of coal and reduced acoustic emissions. Shen et al. [30] studied the acoustic emission characteristics during the hydraulic flushing process of coal seams. The results indicated that the changes in acoustic emission signals were basically consistent with the changes in load and water pressure. Jin et al. [31] studied and proved that there was a highly positive correlation between the plastic strain of coal and the acoustic emission characteristic parameters in the uniaxial compression process of coal and rock. Jia et al. [32] conducted laboratory shear failure tests on sandstone samples to study the laws of electromagnetic and acoustic signals. The results indicated that when the main fault occurred, the correlation between magnetic signals and stress and acoustic emission signals was strong. Li et al. [33] calculated the fractal dimension of each loading step by using the AE count rate data and the phase space reconstruction theory. The results showed that the AE count rate can effectively reflect the load during the failure process.

It can be seen that many scholars have made many important achievements in the research of coal and gas outbursts. However, the research is mainly focused on the development stage of outbursts, and there are still some deficiencies in the research on the whole process of outbursts. In addition, there is only a single analysis of acoustic emission parameters, lacking a coupling analysis between acoustic emission and other parameters. Therefore, the physical experiment of a coal and gas outburst was carried out, and the acoustic emission and gas pressure were monitored during the whole process of the outburst. The acoustic-gas coupling evolution characteristics in the whole process of outbursts were studied, which is of great significance for monitoring and preventing coal and gas outbursts and ensuring safe production in coal mines.

2. Experimental Method

2.1. Test Equipment

The outburst experiment was carried out with self-developed large-scale multifunctional equipment [34]. The device consists of a coal sample box, a triaxial loading system, a fast coal uncovering system, a PCI-2 acoustic emission sensor system, and a data acquisition system (Figure 1). The size of the coal specimen is 1050 × 410 × 410 mm. The installation position of the acoustic emission sensor and the gas pressure sensor in this experiment is shown in Figure 2. In order to monitor accurate data, the acoustic emission sensor and the gas pressure sensor are arranged near the outburst mouth, considering that the outburst hole near the outburst mouth is the location where the coal is severely damaged.

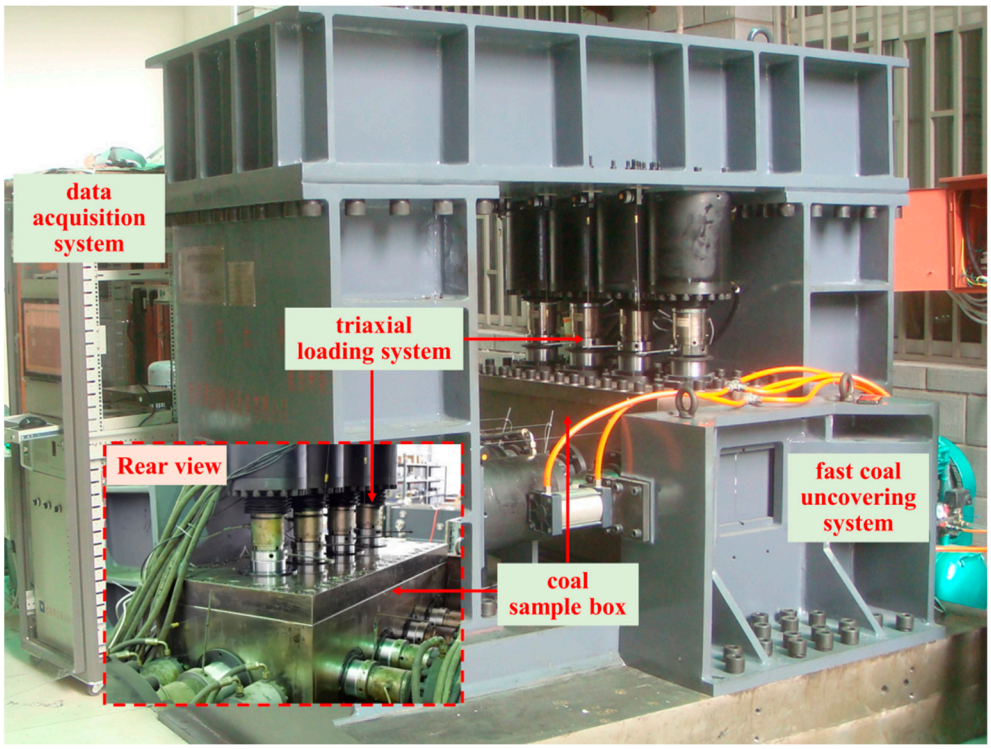

Figure 1. Physical picture of the large-scale multifunctional equipment.

2.2. Test Scheme

The selected coal sample was collected from the K1 coal seam in Sanhui No. 1 Mine of Chongqing Tianfu Mining Co., Ltd. (Chongqing, China). Due to the large size of the specimen box and the large amount of adsorbed gas, CO_2 was used for the test considering the safety problem [35,36], and the gas pressure was 1.0 MPa. The vertical stress of the coal mine was 23 MPa, the stress concentration factor was 1.5, and the later pressure coefficient was 0.6 [37]. Considering that the stress similarity constant was 12, the maximum principal stress in the test was 2.0, 3.0, 3.0, and 1.0 MPa, the intermediate principal stress was 2.0 MPa,

and the minimum principal stress was 1.2, 1.8, 1.8, and 1.0 MPa, respectively, as shown in Table 1.

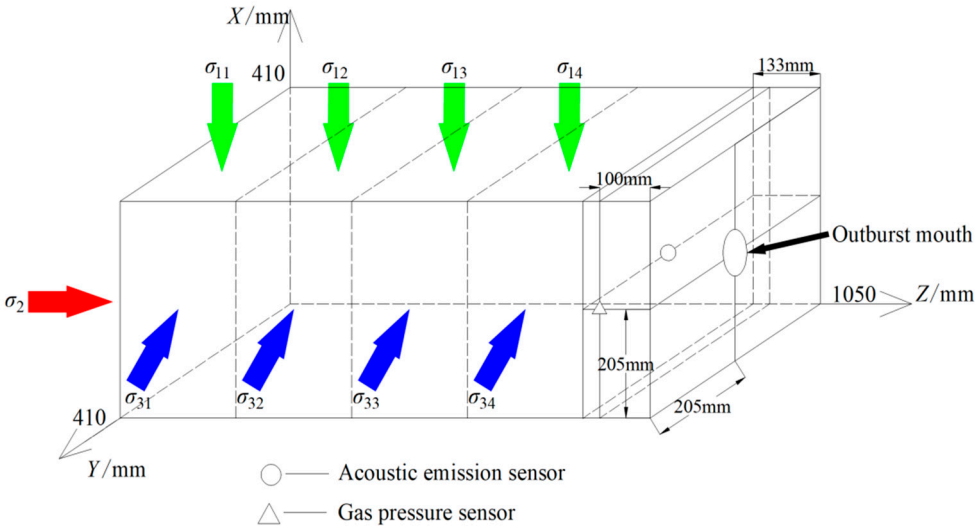

Figure 2. The schematic diagram of sensor installation position.

Table 1. Experimental scheme for coal and gas outburst.

Maximum Principal Stress σ_1 (MPa)				Intermediate Principal Stress σ_2 (MPa)	Minimum Principal Stress σ_3 (MPa)				Gas Pressure P (MPa)
σ_{11}	σ_{12}	σ_{13}	σ_{14}		σ_{31}	σ_{32}	σ_{33}	σ_{34}	
2.0	3.0	3.0	1.0	2.0	1.2	1.8	1.8	0.6	1.0

2.3. Test Procedures

Based on the actual occurrence process of coal and gas outbursts, the whole process of the outburst experiment is divided into three stages, namely the preparation stage, the gestation stage, and the development stage. The specific experimental steps are as follows:

① The preparation stage: Select the coal powders required for the experiment to prepare the coal sample [38,39]. Fill them into the coal sample box and then perform stress molding. Use the vacuum machine to vacuum the coal sample, and then apply stress loading.

② The gestation stage: After a period of stable stress loading, open the cylinder valve and start filling with gas for 48 h. After the first inflation pressure reaches 1.0 MPa, close the cylinder valve for 4 h, and then open the cylinder valve again. Repeat this cycle until inflation lasts for 48 h, and finally close the cylinder valve.

③ The development stage: Clean the site and check whether all sensors operate normally. Adjust the collection frequency of the data collection system. Open the outburst door to induce a coal and gas outburst. Record and collect the experimental data during the whole process of the outburst.

3. Results and Discussion

The evolution of gas pressure and acoustic emission with time in the whole process of outburst is shown in Figure 3. As can be seen from the figure, the acoustic emission signal and gas pressure of coal show different evolution laws at different stages. During the preparation stage, the acoustic emission is mainly concentrated in the stress loading process from 2 to 2.5 h, and the gas pressure is always less than 0, showing a downward trend. The gestation stage is a process with the longest duration, from 3 to 51 h. The acoustic emission in this stage is mainly concentrated after gas adsorption, mainly concentrated in 3~4.8 h, 6~12.4 h and 25.9~35.9 h. The development stage has the shortest duration, with

approximately 20 s. The acoustic emission rises from a small amount to tens of thousands instantly; however, the gas pressure decreases rapidly from 1 MPa to 0. There is also a certain relationship between gas pressure and acoustic emission at each stage, which will be analyzed in detail below.

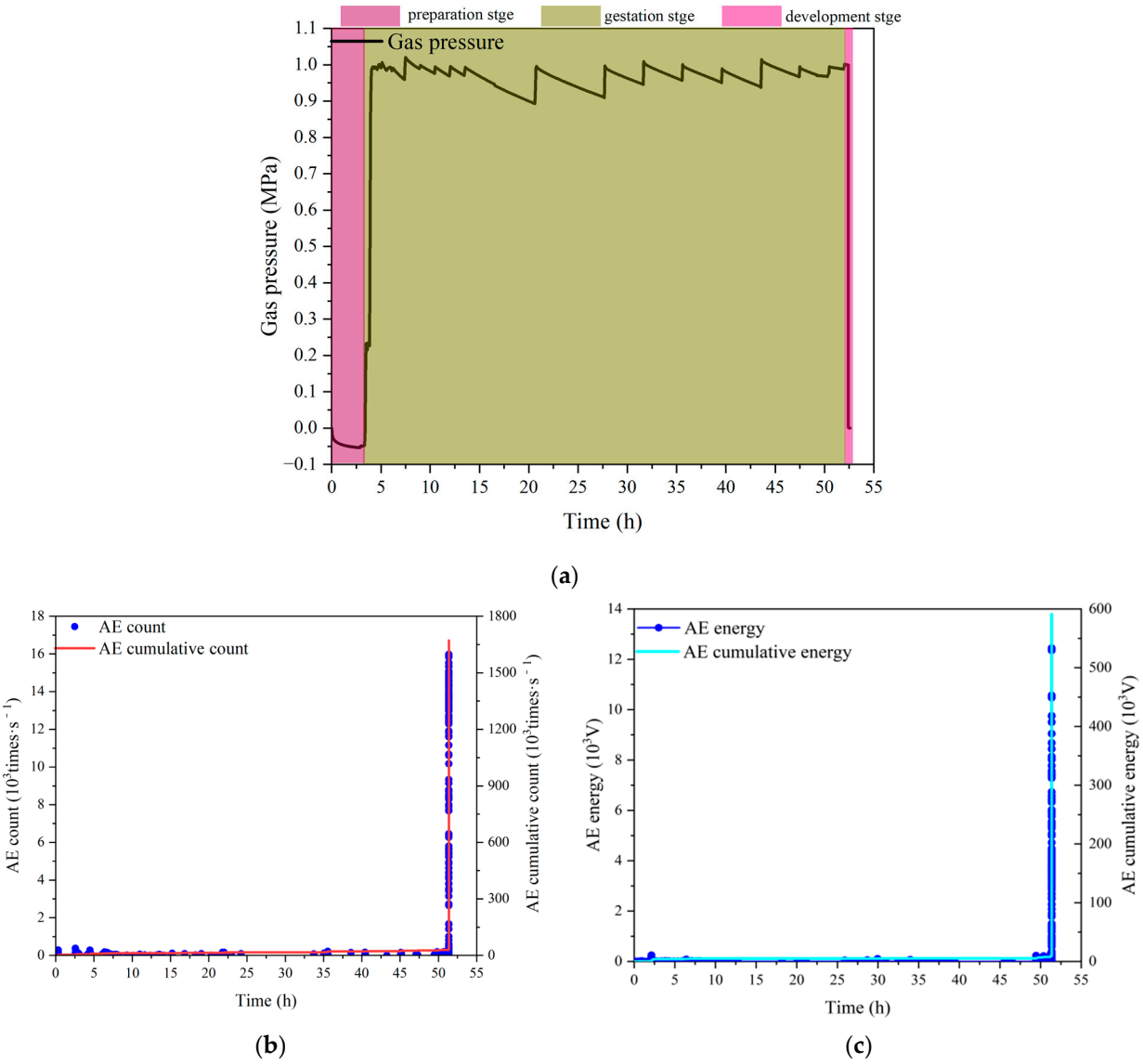

Figure 3. Evolution of gas pressure and acoustic emission with time in the whole process of outburst. (**a**) gas pressure; (**b**) AE count and AE cumulative count; (**c**) AE energy and AE cumulative energy.

3.1. The Outburst Preparation Stage

Figure 4 shows the variation in AE parameters and gas pressure with time during the preparation stage. As can be seen from Figure 4a, a large number of acoustic emission signals appear in two time periods, namely 0~0.59 h and 2.06~2.83 h, respectively. Among them, the acoustic emission has the most signals during 2.06~2.83 h, with a peak count of 285 times·s^{-1}. The peak count during 0~0.59 h is 51 times·s^{-1}, which is only 17.9% of 285 times·s^{-1}. Meanwhile, the cumulative AE count of the outburst preparation stage reaches 23,401 times·s^{-1}. Figure 4b shows the relationship between AE energy, AE cumulative energy, and gas pressure with time. During this stage, AE energy fluctuates slightly before 2.07 h and apparently increases during 2.07~2.83 h. The peak AE energy reaches 245 V, and the cumulative energy of AE in the whole vacuum loading stage reaches 4051 V.

As the vacuum machine continues to vacuum the coal body, the gas pressure gradually decreases during this stage, then increases slightly and remains below 0.

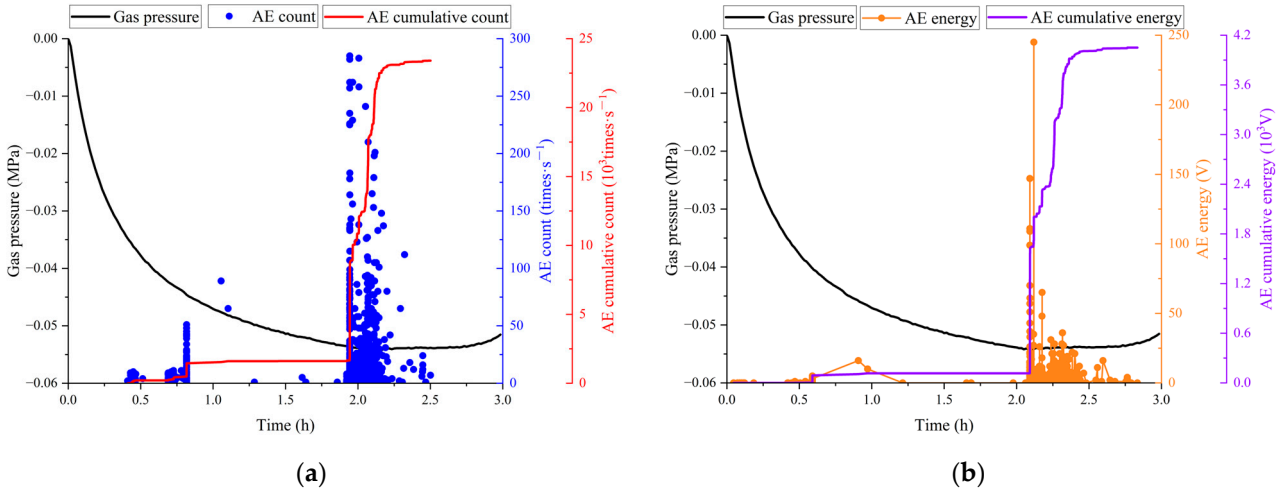

(**a**) (**b**)

Figure 4. Acoustic emission and gas pressure in the process of outburst preparation stage. (**a**) AE count, AE accumulative count, and gas pressure; (**b**) AE energy, AE cumulative energy, and gas pressure.

From Figure 4a, it can be seen that when the gas pressure reaches −0.01 MPa, the acoustic emission signals begin to increase. This is because the gas in coal pores flows under the action of a pressure gradient, and the coal particles are rearranged. Meanwhile, a small amount of air attached to the coal detaches from the constraints of the coal particles, resulting in some microcracks. Therefore, a small number of acoustic emission signals are generated. The coal body maintains a certain degree of stability from −0.01 to −0.035 Mpa, and there are no obvious acoustic emission signals. When the gas pressure ranges from −0.35 to −0.4 Mpa, the acoustic emission signals increase sharply, mainly because continuous vacuum pumping leads to the dislocation of some coal particles. The stress is applied to the coal after 2.1 h, and the coal body is compressed. The primary cracks in coal become smaller or closed; therefore, a large number of acoustic emission signals are generated. In Figure 4b, there is little AE energy generated before the gas pressure decreases to −0.04 Mpa. However, AE energy begins to increase sharply after 2 h because of the compression of the coal sample. The results prove that the main reason for acoustic emission during the outburst preparation stage is stress loading. Overall, there is no direct correlation between gas pressure and acoustic emissions during the outburst preparation stage. The degree of damage to the coal is not high when vacuuming, and the acoustic emission signal is less. Some acoustic emission signals are generated during the stress loading of coal. Therefore, the stress loading during the preparation stage is the main factor leading to changes in coal seam parameters.

3.2. The Outburst Gestation Stage

Among the three stages of coal and gas outburst, the gestation stage has the longest duration, reaching 48 h, as shown in Figure 5. When the coal seam is aerated, the gas pressure rapidly increases. When the gas pressure reaches the predetermined value of 1 MPa for the first time, stop inflating. Thus, the coal seam adsorbs gas, and the gas pressure begins to decrease. After the gas pressure drops to around −0.9 MPa, continue to inflate to the predetermined value, then stop and continue cycling this operation until gas adsorption equilibrium.

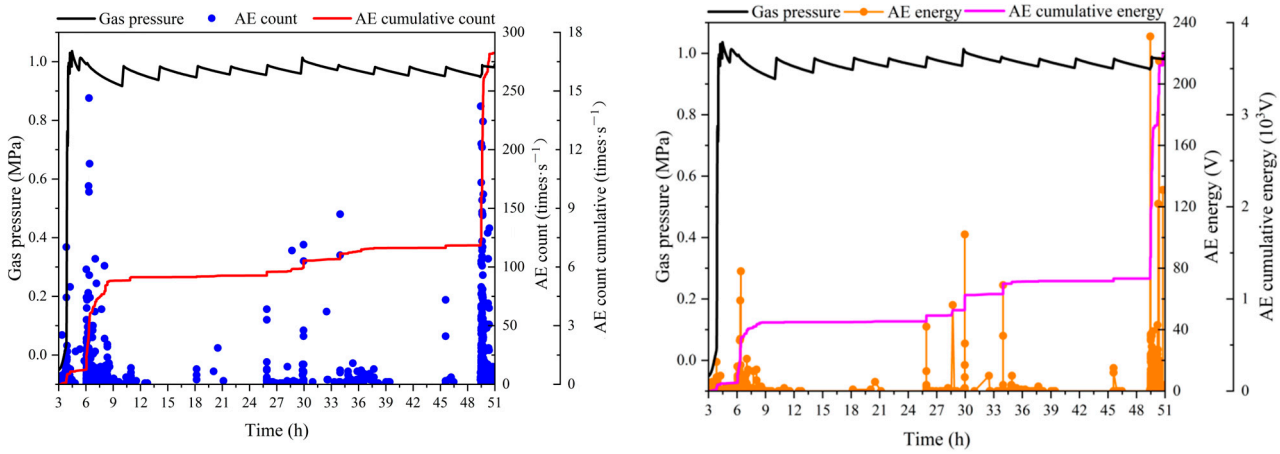

(**a**) (**b**)

Figure 5. Acoustic emission and gas pressure in the process of outburst gestation stage. (**a**) AE count, AE accumulative count, and gas pressure; (**b**) AE energy, AE cumulative energy, and gas pressure.

As can be seen from Figure 5a, a large number of acoustic emission counts are generated throughout the entire gestation stage. The main generation of acoustic emission signals is divided into four time periods. The first time period is from 3 to 4.8 h, and the peak value of the AE count during this time period is 117 times·s^{-1}. As the gas pressure continues to increase, the amount of gas adsorbed by coal also continues to increase. The increase in the amount of adsorbed gas in coal fractures leads to an increase in fractures, causing microfractures of coal particles, and the coal body generates acoustic emission signals that gradually increase. The second time period is from 6 to 12.7 h. During this period, a large number of acoustic emission signals will also be generated. The peak value of the AE count reached 265 times·s^{-1}, which is the largest peak in three time periods. The acoustic emissions generated during this period are mainly caused by the stress of coal unloading rather than gas inflation. The third time period is from 25.9 to 35.9 h. The peak value of the AE count reaches 145 times·s^{-1}. The source of acoustic emissions during this time period is the sudden increase in gas adsorption capacity when the gas cylinder is opened again for inflation. From the entire process of gas filling and adsorption, it can be seen that there are fewer acoustic emission signals generated when coal adsorbs gas. There are many acoustic emission signals generated during the gas inflation process, while fewer acoustic emission signals are generated when the inflation is stopped for adsorption. The fourth time period is from 49.1 to 51 h, with a peak AE count of 237 times·s^{-1}. At this point, the adsorption of gas by the coal is basically complete. Then, the stress is loaded again, and preparations are made for the outburst. The loaded stress causes compression and contraction inside the coal body, resulting in a large number of AE counts. As shown in Figure 5b, the AE energy also shows significant changes during these four time periods. The variation pattern of AE energy starts at the adsorption stage and rises. Then there is a significant increase during unloading stress, with a slight increase in the midterm. The most significant change occurs in the fourth time period. At this point, the stress is applied, causing continuous shrinkage of the coal body, resulting in the highest AE energy.

3.3. The Outburst Development Stage

3.3.1. Evolution Characteristics of Gas Pressure and Acoustic Emission

The outburst development stage is the stage where a huge number of acoustic emission signals are generated and the gas pressure changes instantaneously. However, it is the most short-lived process. The change in gas pressure is only 10 s. The generation time of acoustic emission signals is longer than the that of gas pressure changes. In order to analyze the coupling law of acoustic emission and gas pressure more accurately and finely,

four processes with significant fluctuations were selected for segmented analysis based on the changes in gas pressure during 10 s, as shown in Figure 6.

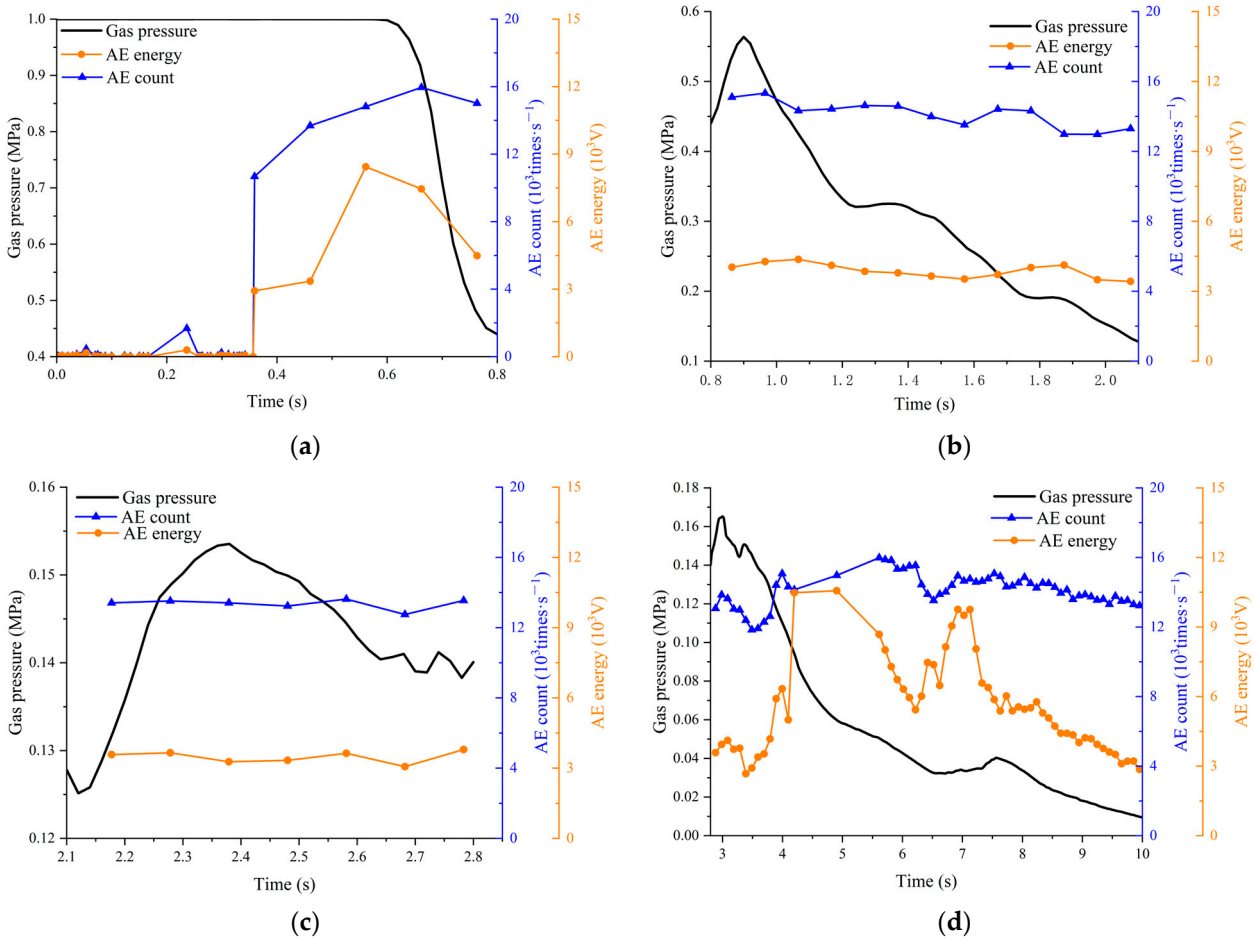

Figure 6. Gas pressure and acoustic emission parameters at development stage. (**a**) Phase I; (**b**) Phase II; (**c**) Phase III; (**d**) Phase IV.

In phase I, the gas pressure does not change immediately after opening the outburst door and remains about 1 MPa. After 0.6 s, the gas pressure begins to drop in a straight line from 1 Mpa to 0.439 Mpa within 0.8 s, with a decrease of 56.10%. This is because after the sudden opening of the outburst door, the coal seam is destroyed by the expansion energy of gas and the elastic energy of coal in the stress relief zone and stress concentration zone. Under the action of gas expansion work, the pulverized coal quickly moves towards the outburst mouth and sprays out from the outburst mouth. As the coal powder is sprayed out, a large amount of gas near the outburst mouth is desorbed, resulting in a rapid decrease in gas pressure. At the same time, the acoustic emissions begin to generate after opening the outburst door for 0.35 s. The AE count reaches a peak of 15,953 times·s^{-1} at 0.66 s, which is also the peak value of the entire outburst development stage. Then there is a slight decrease, reaching 15,009 times·s^{-1} at the end of the phase I. The AE energy reaches a peak of 8437 V at 0.56 s, indicating that the coal seam suffers the greatest degree of damage at this time point. Finally, the AE energy drops to 4485 V, accounting for only 53.15% of the peak value. From the overall perspective of phase I, the change in acoustic emission is earlier than that of gas pressure, and there is an opposite relationship between gas pressure and acoustic emission. As the gas pressure gradually decreases, both the AE count and AE energy reach their peaks.

In phase II, the coal and gas outburst is still ongoing. However, the gas pressure does not continuously decrease but experiences three upward processes. During the first upward

process, the gas pressure rises from 0.439 to 0.563 Mpa after 0.8 s, with an increase of 28.24%. During the second upward process, the gas pressure rises from 0.320 to 0.325 Mpa after 1.24 s, with an increase of 1.56%. During the third upward process, the gas pressure rises from 0.190 to 0.191 Mpa after 1.8 s, with an increase of 0.52%. The reason is that with the continuous development of outbursts, broken coal blocks the outburst mouth, and coal powder cannot be sprayed out in a short period of time. However, a large amount of gas is still being desorbed, leading to a gradual increase in gas pressure inside the outburst hole. When the gas pressure reaches a certain level, the outburst mouth opens again, triggering a new round of the outburst process, and the gas pressure drops again. The phenomenon is also known as the intermittent development of coal and gas outbursts [40]. Overall, the gas pressure in the coal seam shows a decreasing trend, and there is still a large amount of acoustic emission from the continuous destruction and ejection of coal. The AE count is above 12,900 times·s^{-1}, and the peak value is 15,327 times·s^{-1} at 0.96 s, while the AE energy remains above 3400 V, and the peak value is 4365 V at 1.06 s.

In phase III, the gas pressure initially shows an upward trend and then decreases again. From 2.12 s to 2.38 s, the gas pressure increases from 0.125 Mpa to 0.153 Mpa, for an increase of 18.66%. The second rise is from 2.64 s to 2.68 s, and the gas pressure increases from 0.140 Mpa to 0.141 Mpa, with an increase of only 0.71%. The last rise is from 2.72 s to 2.74 s, and the gas pressure increases from 0.138 Mpa to 0.141 Mpa, with an increase of 2.17%. The comparison shows that the first increase in gas pressure has the highest range, followed by the third, and finally the second. Therefore, the amount of gas desorption is not decreasing gradually, which is a fluctuating process, and the overall trend of gas pressure changes in phase III is similar to that in phase II. In addition, the AE count remains at 12,749 times·s^{-1} and above, reaching a peak value of 13,625 times·s^{-1} at 2.58 s. The generation of AE energy is also relatively stable; it is maintained above 3000 V and reaches a peak value of 3796 V at 2.78 s. In summary, the acoustic emission signals are still being generated, and the gas pressure presents a fluctuating trend of rising and falling, indicating that the coal seam is still continuing to rupture in this phase.

Phase IV is the final phase of gas pressure changes in the process of the outburst development stage, and it is also the process where the gas pressure changes the longest over time. The gas pressure rose for the first time to 0.165 Mpa at 3 s, with an increase of 17.85%. The second rise occurred between 3.28 s and 3.36 s, and the gas pressure rose from 0.144 Mpa to 0.150 Mpa, an increase of 4.16%. The last increase is between 7.06 s and 7.56 s, reaching 0.40 Mpa, with an increase of 21.21%. At this time, the gas energy in the stress relief zone and stress concentration zone is greatly consumed. Due to the lack of gas supply supplementation, the gas pressure during the outburst process tends to steadily decrease and no longer rise. At the same time, the AE count changes slightly while the AE energy begins to rapidly increase after 4 s. On the whole, the AE count remains above 12,000 times·s^{-1}, and the AE energy remains above 3000 V. In phase IV, the gas pressure still maintains a downward trend while the acoustic emission signal fluctuates, indicating that the failure rate of coal seams changes with time. The fluctuation of gas pressure begins to slow down, indicating a decrease in gas desorption in the coal seam. While the acoustic emission signals are still being produced in large quantities, indicating that the coal seam is still being destroyed. Therefore, from the perspective of the acoustic-gas coupling law, the acoustic emission signals can more accurately reflect the damage state of the coal seam in the late stage of outburst development.

3.3.2. Quantitative Analysis of Acoustic Emission

In the outburst development stage, the time required for the gas pressure to gradually change from 1 Mpa to stabilize is 10 s. At this time, the acoustic emission signal from the coal seam is still continuously generated in large quantities. Therefore, in response to this situation, the acoustic emission signal is analyzed separately and systematically, as shown in Figure 7.

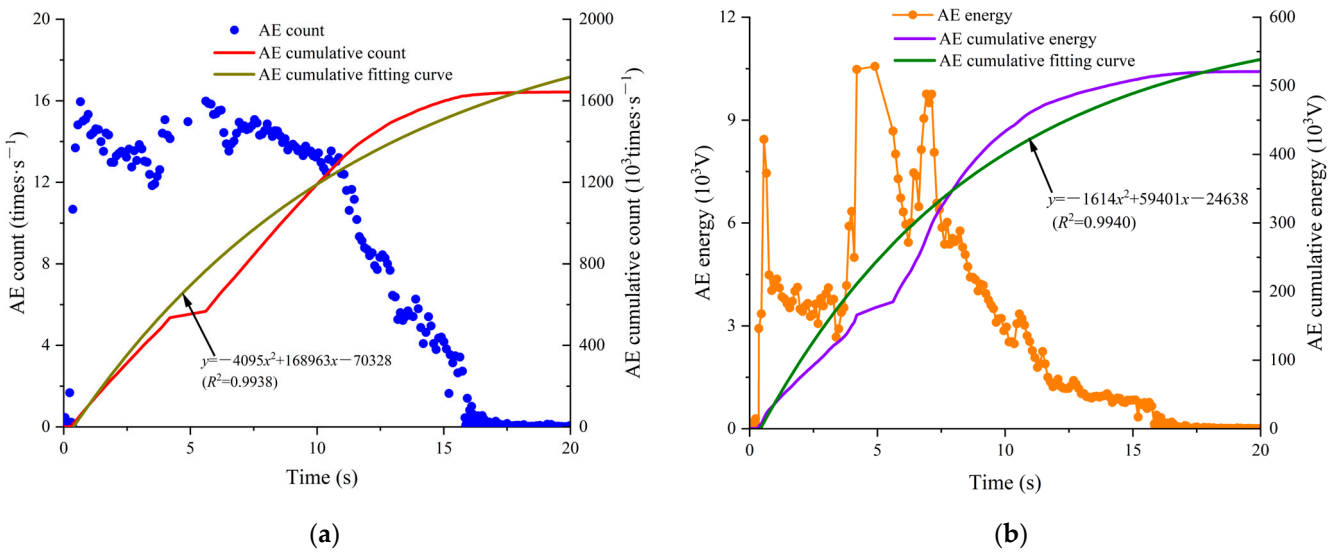

(**a**) (**b**)

Figure 7. Acoustic emission evolution in the outburst development stage. (**a**) AE count, AE cumulative count, and fitting curve; (**b**) AE energy, AE cumulative energy, and fitting curve.

Figure 7a shows the changes in AE count, AE cumulative count, and fitting curve over time. At the moment of opening the outburst door, the AE count immediately rises to around 16,000 times·s^{-1}, then there is a slight decrease. It begins to rise again after 4 s, reaching a peak value similar to the moment when the outburst door is just opened. Then the AE count began to slowly decrease again. When the fall time reaches 10 s, the gas pressure begins to stabilize. When the time exceeds 10 s, the decrease in AE count accelerates, and there is no obvious signal after 16 s. This indicates that there is no significant change in gas pressure after 10 s, however, the coal seam is still damaged. This damage is caused by gas desorption, but the gas desorption amount is small, which is not enough to cause the coal powder to be ejected again. In contrast, the rate of rise of the AE cumulative count curve is relatively flat. Therefore, the AE cumulative count curve with time is fitted, which follows a parabolic relationship, namely, $y = -4095x^2 + 168{,}963x - 70{,}328$ ($R^2 = 0.9938$). It can be seen that the trend of the AE cumulative count curve is basically consistent with the variation pattern of the fitted parabolic curve. Thus, the fitting parabola curve can be used to directly represent the AE cumulative count curve, and the cumulative count of AE at each moment can be calculated to constantly grasp the changes in acoustic emission of coal during the outburst process.

Figure 7b shows the changes in AE energy, AE cumulative energy, and the fitting curve over time. Overall, there are three AE energy peaks in the whole process. Comparing with Figure 7a, it can be seen that at the first peak of AE counting, the AE energy does not reach its peak. At the second peak of AE counting, the AE energy reached its peak value of 10,500 V. The variation trend of AE cumulative energy is similar to the AE cumulative count. Therefore, the AE cumulative energy curve with time is also fitted by the parabolic relationship, namely, $y = -1614x^2 + 59{,}401x - 24{,}638$ ($R^2 = 0.9940$). As a result, the cumulative acoustic emission signal at each time point during the outburst development stage can be calculated and predicted.

3.4. Comparative Analysis of Acoustic Emission at Different Stages

According to the acoustic emission characteristics of different stages in the whole process of coal and gas outburst analyzed above, the AE cumulative count, AE cumulative energy, and their peak values are summarized as shown in Table 2.

Table 2. Statistical data on acoustic emission.

Different Stage	AE Count Peak (Times·s^{-1})	AE Cumulative Count (Times·s^{-1})	AE Energy Peak (V)	AE Cumulative Energy (V)
Preparation stage	285	23,401	245	4051
Gestation stage	265	16,959	231	3671
Development stage	15,980	1,642,996	10,566	520,787
Total		1,683,356		528,509

From the table, it can be seen that the most important stage in producing acoustic emissions is the outburst development stage. The AE count peak reaches 15,980 times·s^{-1} during the outburst development stage, while the outburst preparation stage only accounts for 1.78% and the outburst gestation stage accounts for 1.66%, far lower than the development stage. The AE energy peak is also significantly higher in the outburst development stage than in the first two stages. The outburst preparation stage accounts for 2.31% of the outburst development stage, and the outburst gestation stage accounts for 2.19%. During the entire process of coal and gas outbursts, the total cumulative count of AE reaches 1,683,356 times·s^{-1}. The outburst preparation stage accounts for 1.40% of the total cumulative count, the outburst gestational stage accounts for 1.01% and the outburst development stage reaches 97.59%. Meanwhile, the total cumulative energy of AE reaches 528,509 V throughout the entire process. The outburst preparation stage accounts for 0.77%, the outburst gestation stage accounts for 0.69%, and the outburst development stage accounts for 98.54%. It can be seen from the AE counts peak and cumulative AE counts, as well as the proportion of AE energy peak and AE cumulative energy at different stages, that the outburst development stage is the main stage of acoustic emission generation, which is far greater than the sum of the other two stages. The degree of damage to the coal seam during this stage is also the greatest, and it is the most important stage in the entire process of coal and gas outburst.

4. Conclusions

In order to have a more accurate understanding of the occurrence and disaster process of an outburst accident, the physical simulation test of the whole process of an outburst accident was carried out by self-developed large-scale multifunctional equipment, and the gas pressure and acoustic emission of the coal seam were monitored throughout the entire process.

(1) The gas pressure drops and the AE amount produced are relatively small during the preparation stage, and there is no direct correlation between them. The gestation stage is the longest, with continuous fluctuations after a rapid increase in gas pressure, and the AE amount is mainly concentrated in the process of gas inflation. The development stage has the shortest duration with the greatest changes in gas pressure and acoustic emissions, and it has a strong coupling evolution law.

(2) The development stage is divided into four phases. The generation of acoustic emissions in phase I occurs earlier than the change in gas pressure. In phase II, the gas pressure fluctuates significantly and continues to generate acoustic emissions. In phase III, the outburst is still ongoing, and the desorption of adsorbed gas causes fluctuations in gas pressure. In phase IV, the gas pressure drops to atmospheric pressure, and the AE signal still maintains a large amount of production.

(3) During the entire process of an outburst, there are significant differences in acoustic emission signals among different stages. The AE count peak during the development stage is 15,980 times·s^{-1}, while the preparation stage is 285 times·s^{-1} and the gestation stage is 265 times·s^{-1}. The AE energy peak values during the preparation stage, gestation stage, and development stage are 245 V, 231 V, and 10,566 V, respectively. The cumulative count of AE reaches 1,683,356 times·s^{-1}, with the preparation stage, gestation stage, and development stage being 1.40%, 1.01%, and 97.59%, respectively.

(4) To summarize, the outburst development stage is the main stage of acoustic emission generation and is far greater than the sum of the other two stages. Moreover, the

evolution of the AE cumulative count and cumulative energy over time follows a parabolic equation. Therefore, during coal production, the outburst can be monitored through gas pressure in the preparation stage and gestation stage. Once in the development stage, more sensitive signals of AE and their fitting results are used for outburst hazard monitoring and early warning to improve the safety level of coal mine production.

Author Contributions: Data curation, C.Z. and J.X.; funding acquisition, C.Z.; investigation, W.Z. and S.P.; methodology, C.Z., J.X. and S.P.; validation, C.Z. and S.Y.; visualization, W.Z. and S.Y.; writing—original draft, W.Z.; writing—review and editing, C.Z., Q.J. and M.L. All authors have read and agreed to the published version of the manuscript.

Funding: This work was supported by the National Key R&D Program of China (No. 2022YFC3004701), the National Natural Science Foundation of China (No. 52274242, No. 51904293), and the Jiangsu Funding Program for Excellent Postdoctoral Talent (No. 2022ZB505).

Institutional Review Board Statement: Not applicable.

Informed Consent Statement: Not applicable.

Data Availability Statement: Data are available at chaolinzhang@cumt.edu.cn.

Conflicts of Interest: The authors declare that they have no known competing financial interest or personal relationships that could have appeared to influence the work reported in this paper.

References

1. Zhang, J.; Li, X.; Qin, Q. Study on overlying strata movement patterns and mechanisms in super-large mining height stopes. *Eng. Geol. Environ.* **2023**, *82*, 142. [CrossRef]
2. Liu, S.; Sun, H.; Zhang, D. Experimental study of effect of liquid nitrogen cold soaking on coal pore structure and fractal characteristics. *Energy* **2023**, *275*, 127470. [CrossRef]
3. Zhang, C.; Wang, P.; Wang, E.; Xu, J.; Li, Z.; Liu, X.; Peng, S. Coal and gas outburst mechanism: Research progress and prospect in China over the past 70 years. *Coal Geol. Explor.* **2023**, *51*, 59–94.
4. Zhang, C.; Wang, E.; Wang, Y.; Zhou, X. Spatial-temporal distribution of outburst accidents from 2001 to 2020 in China and suggestions for prevention and control. *Coal Geol. Explor.* **2021**, *49*, 134–141.
5. Wang, F.; Zhang, P.; Cui, B.; Sun, Z.; Zhang, K. Research progress of disaster factors and a prevention alarm index of coal and gas outbursts. *Arab. J. Geo. Sci.* **2021**, *14*, 2042. [CrossRef]
6. Liu, S.; Li, X. Experimental study on the effect of cold soaking with liquid nitrogen on the coal chemical and microstructural characteristics. *Environ. Sci. Pollut. R.* **2023**, *30*, 36080–36097. [CrossRef] [PubMed]
7. Sobczyk, J. A comparison of the influence of adsorbed gases on gas stresses leading to coal and gas outburst. *Fuel* **2014**, *115*, 288–294. [CrossRef]
8. Wang, K.; Du, F. Coal-gas compound dynamic disasters in China: A review. *Process Saf. Environ. Prot.* **2020**, *133*, 1–17. [CrossRef]
9. Jin, K.; Cheng, Y.; Ren, T.; Zhao, W.; Tu, Q.; Dong, J.; Wang, Z.; Hu, B. Experimental investigation on the formation and transport mechanism of outburst coal-gas flow: Implications for the role of gas desorption in the development stage of outburst. *Int. J. Coal Geol.* **2018**, *194*, 45–58. [CrossRef]
10. Zhang, C.; Wang, E.; Li, B.; Kong, X.; Xu, J.; Peng, S.; Chen, Y. Laboratory experiments of CO_2-enhanced coalbed methane recovery considering CO_2 sequestration in a coal seam. *Energy* **2023**, *262*, 125473. [CrossRef]
11. Tang, J.; Hao, N.; Pan, Y.; Sun, S. Experimental study on precursor characteristics of coal and gas outbursts based on acoustic emission energy analysis. *Int. J. Rock Mech. Rock Eng.* **2021**, *40*, 31–42.
12. Fu, G.; Xie, X.C.; Jia, Q.S.; Tong, W.Q.; Ge, Y. Accidents analysis and prevention of coal and gas outburst: Understanding human errors in accidents. *Process Saf. Environ. Prot.* **2020**, *134*, 1–23. [CrossRef]
13. Skochinski, A.A. Communication of the initiation of a sudden outburst of gas and coal in the model in outburst laboratory of the Institute of Mining of AN SSSR. *Ugol* **1953**, *10*, 39.
14. Alexeev, A.D.; Revva, V.N.; Alyshev, N.A.; Zhitlyonok, D.M. True triaxial loading apparatus and its application to coal outburst prediction. *Int. J. Coal Geol.* **2004**, *58*, 245–250. [CrossRef]
15. Zhang, Y.; Cao, S.; Yan, J.; Zhang, Z. Mechanism of coal-gas outburst based on deformed coal. *Min. Miner. Process.* **2007**, 1382–1386.
16. Guo, B.; Li, Y.; Jiao, F.; Luo, T.; Ma, Q. Experimental study on coal and gas outburst and the variation characteristics of gas pressure. *Geomech. Geophys. Geo.* **2018**, *4*, 355–368. [CrossRef]
17. Lu, Z.; Wang, L.; Lv, M.; Lei, Y.; Wang, H.; Liu, Q. Experimental study on coal and gas outburst risk in strong outburst coal under different moisture content. *Front. Earth Sci.* **2022**, *10*, 782372. [CrossRef]

18. Shi, X.; Song, D. Study of the solid-gas-stress coupling model and its application. *Sci. Rep.* **2023**, *13*, 5135. [CrossRef]
19. Ding, Y.; Yue, Z. An experimental investigation of the roles of water content and gas decompression rate for outburst in coal briquettes. *Fuel* **2018**, *234*, 1221–1228. [CrossRef]
20. Xue, S.; Zheng, C.; Zheng, X.; Jiang, B.; Li, Y.; Wang, Z. Experimental determination of the outburst threshold value of energy strength in coal mines for mining safety. *Process Saf. Environ. Prot.* **2020**, *138*, 263–268. [CrossRef]
21. Cao, J.; Dai, L.; Sun, H.; Wang, B.; Zhao, B.; Yang, X.; Zhao, X.; Guo, P. Experimental study of the impact of gas adsorption on coal and outburst dynamics effects. *Process Saf. Environ. Prot.* **2019**, *128*, 158–166. [CrossRef]
22. Zhou, B.; Yang, S.; Wang, C.; Cai, J.; Xu, Q.; Sang, N. Experimental study on the influence of coal oxidation on coal and gas outburst during invasion of magmatic rocks into coal seams. *Process Saf. Environ. Prot.* **2019**, *124*, 213–222. [CrossRef]
23. Yang, W.; Lin, M.; Walton, G.; Lin, B.; Sinha, S.; Lu, C.; Li, T. Blasting-enhanced water injection for coal and gas out-burst control. *Process Saf. Environ. Prot.* **2020**, *140*, 233–243. [CrossRef]
24. Frid, V.; Vozoff, K. Electromagnetic radiation induced by mining rock failure. *Int. J. Coal Geol.* **2005**, *64*, 57–65. [CrossRef]
25. Shen, R.; Qiu, L.; Zhao, E.; Han, X.; Li, H.; Hou, Z.; Zhang, X. Experimental study on frequency and amplitude characteristics of acoustic emission during the fracturing process of coal under the action of water. *Saf. Sci.* **2019**, *117*, 320–329. [CrossRef]
26. Qiu, L.; Song, D.; Li, Z.; Liu, B.; Liu, J. Research on AE and EMR response law of the driving face passing through the fault. *Saf. Sci.* **2019**, *117*, 184–193. [CrossRef]
27. Zheng, J.; Jin, X.; Tian, K.; Zhou, Y. Acoustic emission and damage characteristics of anthracite under different conditions. *Mater Tehnol.* **2021**, *55*, 213–218. [CrossRef]
28. Kong, X.; Wang, Y.; Hu, S.; Shen, R.; Li, X.; Zhan, T. Fractal characteristics and acoustic emission of coal containing methane in triaxial compression failure. *J. Appl. Geophys.* **2016**, *124*, 139–147. [CrossRef]
29. Ali, M.; Wang, E.; Li, Z.; Wang, X.; Kan, N.; Zang, Z.; Alarifi, S.S.; Fissha, Y. Analytical damage model for predicting coal failure stresses by utilizing acoustic emission. *Sustainability* **2023**, *15*, 1236. [CrossRef]
30. Shen, R.; Zhang, X.; Wang, E.; Li, H.; Han, X.; Hou, Z. Application of acoustic emission technique to the evaluation of coal seam hydraulic flushing effect. *Energy* **2019**, *12*, 1705. [CrossRef]
31. Jin, P.; Wang, E.; Song, D. Study on correlation of acoustic emission and plastic strain based on coal-rock damage theory. *Geomech. Eng.* **2017**, *12*, 627–637. [CrossRef]
32. Jia, H.; Niu, Y.; Liu, X.; Wang, E. Study on electric-magnetic-acoustic signal regularity and its correlation during rock shear failure. *Adv. Mater. Sci. Eng.* **2019**, *2019*, 4687607. [CrossRef]
33. Li, D.; Wang, E.; Kong, X.; Wang, X.; Zhang, C.; Jia, H.; Wang, H.; Qian, J. Fractal characteristics of acoustic emissions from coal under multi-stage true-triaxial compression. *J. Geophys. Eng.* **2018**, *15*, 2021–2032.
34. Zhang, C.; Xu, J.; Yin, G.; Peng, S.; Li, Q.; Chen, Y. A novel large-scale multifunctional apparatus to study the disaster dynamics and gas flow mechanism in coal mines. *Rock Mech. Rock. Eng.* **2019**, *52*, 2889–2898. [CrossRef]
35. Du, F.; Wang, K.; Zhang, X.; Xin, C.; Shu, L.; Wang, G. Experimental study of coal–gas outburst: Insights from coal–rock structure, gas pressure and adsorptivity. *Nat. Resour. Res.* **2020**, *29*, 2481–2493. [CrossRef]
36. Ma, Y.; Nie, B.; He, X.; Li, X.; Meng, J.; Song, D. Mechanism investigation on coal and gas outburst: An overview. *Int. J. Miner. Metall. Mater.* **2020**, *27*, 872–887. [CrossRef]
37. Zhang, C.; Wang, E.; Xu, J.; Peng, S. Research on temperature variation during coal and gas outbursts: Implications for outburst prediction in coal mines. *Sensors* **2020**, *20*, 5526. [CrossRef] [PubMed]
38. Sobczyk, J. The influence of sorption processes on gas stresses leading to the coal and gas outburst in the laboratory conditions. *Fuel* **2011**, *90*, 1018–1023. [CrossRef]
39. Dai, L.; Liu, Y.; Cao, J.; Yang, X.; Sun, H.; Wen, G.; Wang, B. A study on the energy condition and quantitative analysis of the occurrence of a coal and gas outburst. *Shock Vib.* **2019**, *2019*, 8651353. [CrossRef]
40. Miao, F.; Sun, D.; Hu, Q. The formation mechanism of shock waves in the coal and gas outburst process. *J. China Coal Soc.* **2013**, *38*, 367–372.